Non-monotonic dynamical correlations beneath the surface of glass-forming liquids

Hailong Peng,[1, *] Huashan Liu,[1] and Thomas Voigtmann[2, 3, †]

[1]*School of Materials Science and Engineering, Central South University, 932 South Lushan Rd, 410083 Changsha, China*
[2]*Institut für Materialphysik im Weltraum, Deutsches Zentrum für Luft- und Raumfahrt (DLR), 51170 Köln, Germany*
[3]*Department of Physics, Heinrich-Heine-Universität Düsseldorf,*
Universitätsstraße 1, 40225 Düsseldorf, Germany
(Dated: October 5, 2022)

Collective motion over increasing length scales is a signature of the vitrification process of liquids. We demonstrate how distinct static and dynamic length scales govern the dynamics of vitrifying films. In contrast to a monotonically growing static correlation length, the dynamical correlation length that measures the extent of surface-dynamics acceleration into the bulk, displays a striking non-monotonic temperature evolution that is robust also against changes in detailed interatomic interaction. This non-monotonic change defines a cross-over temperature T_* that is distinct from the critical temperature T_c of mode-coupling theory (MCT). We connect this non-monotonic change to a morphological change of cooperative rearrangement regions (CRR) of fast particles, and to the point where the decoupling of fast-particle motion from the bulk relaxation is most sensitive to fluctuations. We propose a rigorous definition of this new cross-over temperature T_* within a recent extension of MCT, the stochastic β-relaxation theory (SBR).

Dynamical processes in a liquid close to the glass transition become cooperative across spatial regions of increasing extent [1], and it is thus natural to seek an intrinsic correlation length whose divergence would signal the transition. Yet, the hallmark of the glass transition is a dramatic change in the dynamics that is caused by only weak changes in the statics. Consistently, attempts at defining *static* correlation lengths have found them to change only weakly close to the (computationally or experimentally accesible part) of the transition [1–4]. Only recently it has become clear that in certain perturbed systems, *dynamic* correlation lengths can be defined that display a much more interesting, non-monotonic behavior [5–7] with a peak at some cross-over temperature.

The prevailing methodology to detect spatial correlations in glassy systems is suggested by the random first-order theory (RFOT) [8–10]: pinning a subset of particles in the equilibrium fluid, one examines how the configuration of the rest of particles is influenced [11–15]. While this point-to-set (PTS) protocol is designed to keep the *static* properties of the system in equilibrium, it represents a strong perturbation of the dynamics [16, 17]: The freezing of some particles can be viewed as imposing a zero-temperature region and hence a strong temperature gradient, yet the associated linear-response regime shrinks to zero at the glass transition [18]. Since non-monotonic variations appear more broadly in the non-equilibrium dynamics of glass formers [19, 20], this questions whether non-monotonic changes also appear in the equilibrium dynamics.

We demonstrate here that the study of glass-forming fluids with a free surface offers a clean way to interrogate spatio-dynamical correlations *in equilibrium*. The study of glassy films *per se* is an important topic in material

sciences, e.g., for the fabrication of ultra-stable glasses [21–23]. We provide here a link of the dynamics in (free-standing) films to the fundamental features of the glass transition in the bulk.

In particular we find that the dynamics in *fully equilibrated films* is governed by a non-monotonic dynamical correlation length. We demonstrate that the cross-over temperature T_* of maximal dynamical correlations also governs the shape transition of cooperative rearrangement regions (CRR) of fast particles in the bulk liquids. This new cross-over point is rationalized in the context of stochastic β-relaxation theory (SBR), as the point where the effect of long-range fluctuations is the most pronounced in the decoupling of fast-particle dynamics from bulk relaxation.

We study two exemplary glass formers by molecular dynamics (MD) simulations: the Kob-Andersen Lennard-Jones binary mixture (LJBM) [24], and a model of the molten CuZr alloy with embedded-atom method (EAM) many-body interactions [25]. Simulations (using the LAMMPS package [26]) start in the bulk liquid at high temperature ($T = 0.6$ for LJBM; $T = 2000\,\mathrm{K}$ for CuZr) and zero pressure. A liquid-vacuum interface was created by an instantaneous increase of the box length along the z-axis [see the illustration in Fig. 1(a)]. After re-equilibration, the membranes were cooled down to the target temperatures in the canonical ensemble (NVT); data was collected in the microcanonical ensemble (NVE) over 16 realizations per state point. To check finite-size effects, we compare simulations of two system sizes: small systems (S) with $L_x = L_y \approx 13\sigma$, $L_z \approx 31\sigma$ and at least $N = 5000$ particles; and large systems (L) with $L_z \approx 40\sigma$ and at least $N = 7000$ particles (where σ is a typical atomic size, $\sigma \approx 2.7\,\text{Å}$ for CuZr; precise information is given in Supplemental Material (SM) [27]).

The spatially resolved dynamics can be assessed through the overlap correlation function suggested by the PTS method [9]: the simulation box is discretized
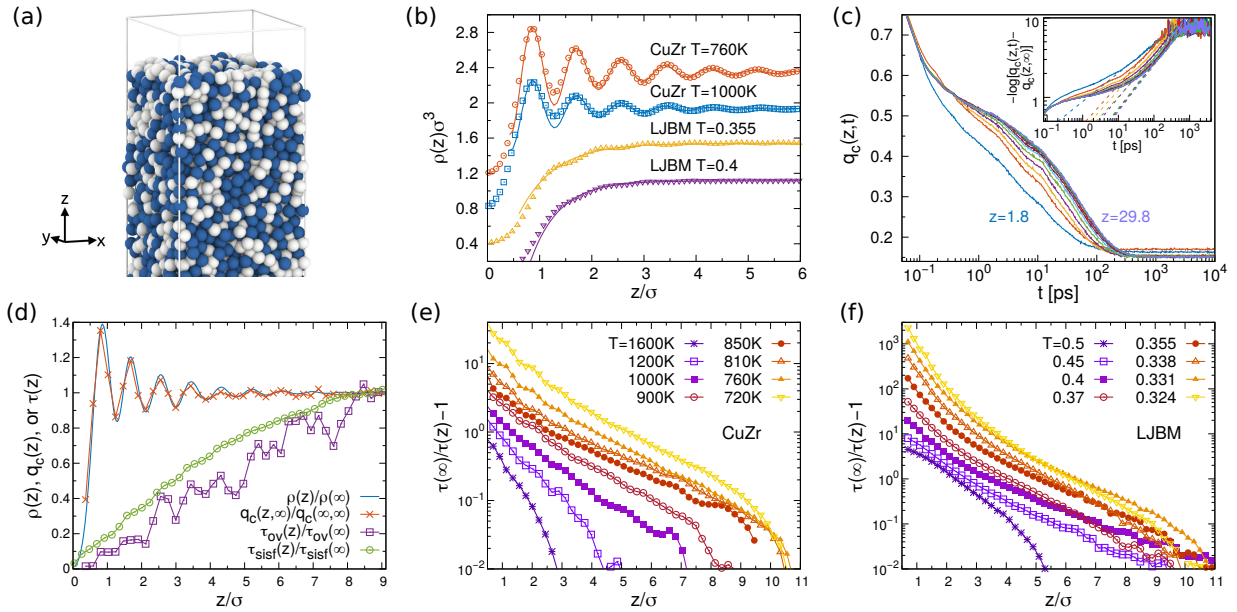

FIG. 1. (a) Snapshot of the simulation setup (CuZr system, colors indicating atomic species). (b) Static density profiles $\rho(z)$ as a function of distance z from the surface along the normal into the bulk, for the CuZr liquid and the Lennard-Jones binary mixture (LJBM) (in units of the average atomic radius σ, each curve shifted vertically in steps of $0.4/\sigma^3$ for clarity). Solid lines are fits to extract the static correlation length. (c) Decay of the overlap correlation function $q_c(z,t)$ (CuZr; $T = 810\,\mathrm{K}$). Dashed lines in the inset exemplify stretched-exponential fits of the structural decay, Eq. (1). (d) Static and dynamic parameters characterizing the overlap correlation function (CuZr; $T = 850\,\mathrm{K}$). The normalized static overlap $q_c(z,\infty)/q_c(\infty,\infty)$ (crosses) follows the normalized density profile $\rho(z)/\rho(\infty)$ (line). The normalized change in the relaxation time $\tau_{\mathrm{ov}}(z)/\tau_{\mathrm{ov}}(0)$ (squares) is shown in comparison to the corresponding quantity obtained from the z-resolved SISF (circles). (e) and (f): Position-dependent relative mobility enhancement $\tau(\infty)/\tau(z) - 1$ (from the layer-resolved SISF) for CuZr and the LJBM.

into small cubic units of size δ (about $0.52\,\sigma \approx 1.4\,\text{Å}$ for CuZr and $0.6\,\sigma$ for the LJBM), and the overlap of configurations a time t apart is calculated as:
$$q_c(z,t) = \left\langle \sum_i n_i(t)n_i(0)\delta\left(z_i - z\right)\right\rangle \Big/ \left\langle \sum_i n_i(0)\delta\left(z_i - z\right)\right\rangle,$$
where $n_i = 1$ if box i at distance z_i from the surface is occupied by an atom and $n_i = 0$ otherwise, and $\langle \cdot \rangle$ denotes an average over the simulation ensemble.

The functions $q_c(z,t)$ follow a standard two-step relaxation pattern of dynamical correlation functions near the glass transition [Fig. 1(c)]: a short-time relaxation to an intermediate-time plateau is followed by stretched-exponential structural relaxation from the plateau. At long times, $q_c(z,t)$ decays to a non-zero z-dependent constant $q_c(z,\infty)$ that represents averaged density fluctuations: the introduction of a free surface induces a static density profile $\rho(z)$ [Fig. 1(b)], and we find $q_c(z,\infty) \propto \rho(z)$ [Fig. 1(d)]. This is the expected behavior for a stationary ergodic system. A *static* correlation length ξ_{stat} characterizes the density profile, extracted from fits of the form $\rho(z) = A(z)\exp(-z/\xi_{\mathrm{stat}}) + \rho(\infty)$, where $\rho(\infty)$ is the density of the bulk liquid. The function $A(z) = A_0 \sin(2\pi(z - z_0)/d_p)$ captures the pronounced surface-induced layering effects seen for CuZr [in Fig. 1(b)]. These are in agreement with experiments on metallic [28] and nonmetallic liquids [29, 30], and grand-canonical MD simulations of liquid films [31]. The LJBM does not show pronounced layering [32], so that there $A(z) = A_0$ is used.

In both cases, the static length scale ξ_{stat} increases monotonically and mildly across the temperature range that we investigate (open symbols in Fig. 2). It qualitatively agrees with standard length scales associated to the bulk dynamics, such as the one extracted from four-point correlation functions [27], as well as with other computer simulation results [1, 3, 11].

To obtain the *dynamical* correlation length, we parametrize the long-time decay of the overlap correlation function by stretched-exponential functions,
$$q_c(z,t) = q_0(z)\exp[-(t/\tau_{\mathrm{ov}}(z))^{\beta(z)}] + q_c(z,\infty), \quad (1)$$
where $\tau_{\mathrm{ov}}(z)$ is a z-dependent relaxation time. Similar $\tau(z)$ are obtained from fits to the collective and self-intermediate scattering function (SISF), or from time-integrals over the correlation functions that provide parameter-free proxies for the structural relaxation time (Fig. 1(d) and SM [27]).

Two spatial regimes emerge in the relative enhancement of the mobility $\mu(z) = 1/\tau(z)$, given by $\tau(\infty)/\tau(z) - 1$, at low temperature [Fig. 1(e,f)]: first, a surface layer extends over the weakly T-dependent static length scale ($z \lesssim 2\sigma$ for CuZr, and 3σ for LJBM), where the density profile is strongly perturbed by the presence of the free surface. We exclude this surface layer from our analysis, separating statically induced variations from purely dynamical ones; this is a crucial dis-
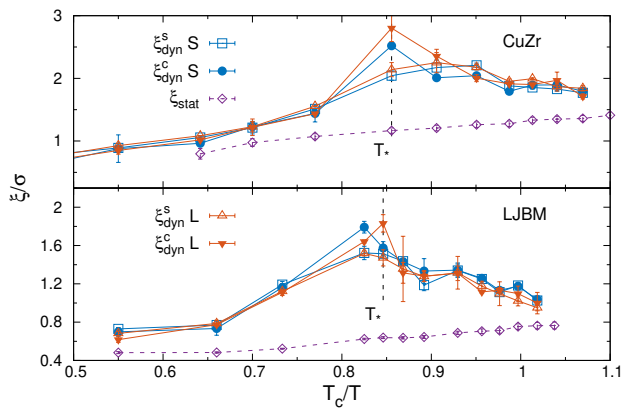
FIG. 2. Temperature dependent statical $\xi_{\text{stat}}(T)$ and dynamical correlation lengths $\xi_{\text{dyn}}(T)$ near a free surface for the CuZr (top panel) and the LJBM liquids (bottom panel). The static correlation length ξ_{stat} is extracted from the exponential decay of $\rho(z)$. Values from the self- ($\xi_{\text{dyn}}^{\text{s}}$) and collective- ($\xi_{\text{dyn}}^{\text{c}}$) intermediate scattering functions are shown in systems of two different sizes (S: small systems; L: large systems). The evolution is non-monotonic around a peak temperature T_* indicated by the dashed vertical lines.

tinction from PTS-based analyses and recent theoretical approaches [33–35] (see SM [27]). More importantly, an intermediate z-range with a much slower decay opens at lower temperatures ($T \lesssim 1000\,\text{K}$ for CuZr, $T \lesssim 0.45$ for LJ). This intermediate regime expands as T is lowered. Here, $\rho(z) \approx \rho(\infty)$, and thus this is the regime where an intrinsic dynamical correlation length ξ_{dyn} can be extracted from the exponential decay of $\mu(z)$, viz.

$$\mu(z) = C \exp[-z/\xi_{\text{dyn}}] + \mu(\infty). \tag{2}$$

Note that this fitting formula differs from the double exponential function utilized in PTS (see SM [27]). One already anticipates from Fig. 1(e–f) that ξ_{dyn} shows a non-monotonic temperature dependence: curves for intermediate temperature (around $T = 850\,\text{K}$ in the CuZr liquid; around $T = 0.4$ in the LJ binary mixture) extend further into the bulk than those both at higher and at lower temperatures.

The resulting dynamical correlation lengths ξ_{dyn} display clear maxima at a temperature T_* (Fig. 2). Both above and below T_*, the dynamic and static (symbols with dashed lines in Fig. 2) correlation lengths become similar. In particular, below T_*, ξ_{dyn} decreases towards the smaller static one, ξ_{stat}, again. This is not a finite-size effect: only around the maximum in ξ_{dyn}, some slight effects of system size (in line with those expected from conventional four-point correlations in supercooled liquids [36–38]) are seen that disappear both at higher and at lower temperatures, and thus give additional evidence that the dynamical correlation length peaks at T_*. In both the CuZr and the LJBM system, we note that the peak observed in ξ_{dyn} over ξ_{stat} is at least a factor of 2. Both systems show very different layering propensity in

the density profiles [Fig. 1(b)] and hence demonstrate the robustness of the maximum in ξ_{dyn} across systems with different surface interactions.

We now demonstrate the intimate link of the maximum in the dynamical correlation length *near the surface* with a cross-over point that governs the *bulk* dynamics. Such a link is remarkable, because the point of maximal correlation length, T_*, is clearly above the T_c of mode-coupling theory (MCT), to which candidates of dynamical changes in the bulk have so far been linked. One example is a change in morphology of the CRR as suggested by RFOT [39].

We identify CRR as nearest-neighbor clusters of fast particles in simulations of the *bulk* systems. Following established procedures [40, 41], fast particles are defined as those that, during the time interval corresponding to the average structural relaxation time, move significantly farther than what is expected from the average mean-squared displacement. Clusters are defined by fast particles initially closer than the first minimum position in the pair distribution function. To quantify the geometric shape of these clusters, we consider the ratio of their correlation length to the expected spherical size: In analogy to percolation theory [42], the average cluster correlation length is given by

$$\xi_{\text{cl}}^2 = \sum_s R_{g,s}^2 s^2 P(s) / \sum_s s^2 P(s), \tag{3}$$

where the sums run over the individual clusters of size s whose probability of occurence is $P(s)$. The radius of gyration of such a cluster is $R_{g,s}^2 = \frac{1}{2s^2} \left\langle \sum_{ij \in s} (\mathbf{r}_i - \mathbf{r}_j)^2 \right\rangle_s$, where $\mathbf{r}$ is the position of particles at the initial time for the considered relaxation time interval. The sum runs over all particles i, j that are part of the cluster, and $\langle \cdots \rangle_s$ denotes the average over all clusters of size s. The expected linear dimension of a spherical cluster of size R_s in turn is defined by $\langle s \rangle = (4\pi/3)\rho_n R_s^3$, where ρ_n is the number density, and $\langle s \rangle = \sum_{s \geq 2} s^2 P(s) / \sum_{s \geq 2} s P(s)$ is the average cluster size. The ratio, ξ_{cl}/R_s, can then be used as a proxy to measure the anisotropy of the fast-particle regions.

As spatial correlations grow with decreasing temperature, ξ_{cl} also grows monotonically [43]. But the aspect ratio of clusters, ξ_{cl}/R_s, evolves non-monotonically [Fig. 3(a)], with a maximum at the same temperature $T_* > T_c$ where also the dynamical correlations show a maximum. Thus we argue that the non-monotonic change in ξ_{dyn} is intimately related to the shape transition of bulk CRR.

Typical shapes of fast-particle clusters in the bulk demonstrate the shape transition [Fig. 3(b–d)]: at high temperatures, clusters are small and of a random-walk like fractal structure. As the temperature is lowered, the clusters increase in size, and at temperatures below T_*, they are relatively compact objects. Around $T = T_*$, the aspect ratio is largest: as the clusters grow in average size upon lowering the temperature, this growth first occurs through a string-like extension of the clusters; only
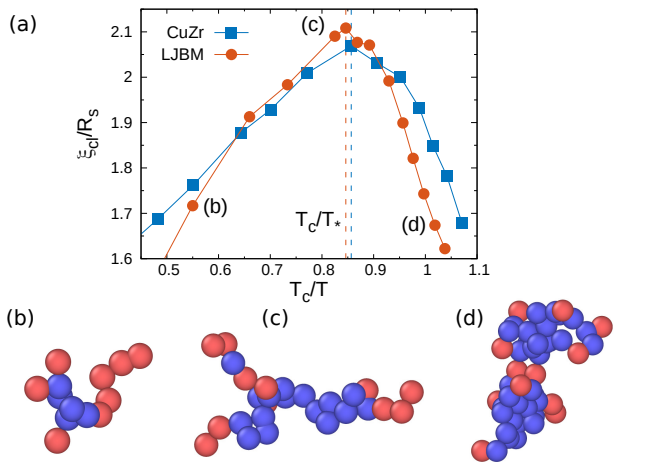
FIG. 3. Characterization of the CRR shape in the bulk liquids. (a) Aspect ratio of fast-particle clusters in the bulk simulations, ξ_{cl}/R_s. Vertical dashed lines are T_* from Fig. 2. (b), (c), and (d), denote the temperature points at which fast-particle clusters are exemplified in the respective panels. Particles in blue correspond to the core of the cluster (having more than two fast nearest neighbours); red particles are those with only one or two fast particles as their nearest neighbors.

FIG. 4. Diffusivity D versus viscosity η for the *bulk* liquids (symbols), compared with the prediction from stochastic β-relaxation theory (solid line, using the MCT exponent parameter $\lambda = 0.75$). CuZr data have been scaled by factors μ_0 and η_0 to match LJ units. Dotted lines are the SBR asymptotes for the SE relation, $D/T \sim \eta^{-1}$, at high temperatures, and a fractional law, $D/T \sim \eta^{-0.56}$, at low temperatures. Red circles mark the MCT-T_c, and T_* predicted from SBR (maximum slope in the inset); arrows indicate the T_* from ξ_{dyn} in Fig. 2.

below T_*, a more isotropic growth of the clusters is seen. While the string-like motion of atoms is well known in supercooled liquids [40, 41, 44, 45], the transition back to more compact (albeit larger) CRR at low temperatures is a more striking result of our study.

Within RFOT the shape change of CRR arises from a competition between string-like particle motion and a free-energy cost associated to the large interfacial area of these strings [39]. However, the shape-transition point was conjectured to be the MCT-T_c, while we find it to be the T_* that was identified in the glassy films. As we show next, it is clearly distinct from T_c and yet rigorously defined within the MCT framework.

The emergence of large CRR signals heterogeneities in the dynamics that *inter alia* lead to a breakdown of the Stokes–Einstein (SE) relation [37, 46–48]: the fast-particle dominated diffusivity decouples from the bulk relaxation that is governed by the slow particles [49, 50]. The stochastic β-relaxation theory (SBR) [51–53], a recent extension of the asymptotic laws of MCT, rationalizes the crossover from regular to fractional SE relations [54], as arising from long-wave length fluctuations in the local dynamical order parameter (see [27] for details). The scaling function of SBR can be evaluated numerically to yield both D and $\eta \sim \tau$, and the result (solid line in Fig. 4) matches the simulation data.

We expect the point of maximal dynamical correlations to be that where changes in the fast-particle dynamics (quantified by the diffusivity) are most sensitive to changes in the bulk dynamics (using viscosity as a proxy). This is indicated by the point where the change in $\delta = \log(D/T)$ with $v = \log(\eta)$ has the strongest sensitivity to control parameters. SBR predicts the derivative
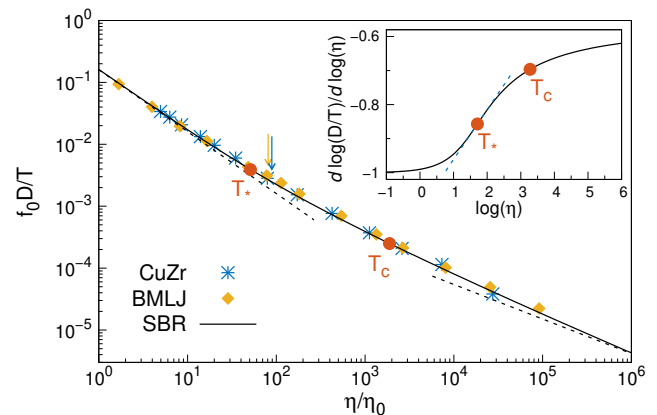
$\epsilon = -d\delta/dv$ to cross over from $\epsilon = 1$ at high temperatures (the ordinary SE relation, $D\eta \sim T$) to an effective exponent $\epsilon = x < 1$ at low temperatures: the fractional SE relation, $D/T \approx \eta^{-x}$, with the exponent x given by the MCT exponent parameter λ [54]. The strongest slope in this cross-over curve (inset of Fig. 4) defines T_* in good agreement with the observed maximum in ξ_{dyn} and the shape transition in the CRR (marked by a circle and arrows, respectively, in Fig. 4). This T_* is strictly higher than T_c because within SBR, non-mean-field fluctuations of the local glassiness have a finite variance and trigger a decoupling of the fast-particle dynamics already above the mean-field T_c.

In conclusion, we find a dynamical correlation length with non-monotonic temperature dependence to govern the dynamics of *equilibrium* free-surface films of glass formers. We demonstrate that the non-monotonic change in dynamical correlations as measured *near the surface* is linked to a non-monotonic shape evolution, i.e., a string-to-compact shape transition, of cooperative rearrangement regions *in the bulk*. This transition occurs at a distinct temperature T_* above the MCT-T_c. It can be identified as the point where the balance of liquid- and glass-like fluctuations in the system is most sensitive to a change in control parameter, and it can be rigorously defined within the recently developed stochastic β-relaxation theory.

[1] L. Berthier and G. Biroli, Rev. Mod. Phys. **83**, 587 (2011).

[2] M. D. Ediger, Annu. Rev. Phys. Chem. **51**, 99 (2000).

[3] E. Flenner, H. Staley, and G. Szamel, Phys. Rev. Lett. **112**, 097801 (2014).

[4] C. Bennemann, C. Donati, J. Baschnagel, and S. C. Glotzer, Nature **399**, 246 (1999).

[5] W. Kob, S. Roldán-Vargas, and L. Berthier, Nat. Phys. **8**, 164 (2012).

[6] G. M. Hocky, L. Berthier, W. Kob, and D. R. Reichman, Phys. Rev. E **89**, 052311 (2014).

[7] K. H. Nagamanasa, S. Gokhale, A. K. Sood, and R. Ganapathy, Nat. Phys. **11**, 403 (2015).

[8] T. R. Kirkpatrick, D. Thirumalai, and P. G. Wolynes, Phys. Rev. A **40**, 1045 (1989).

[9] A. Cavagna, T. S. Grigera, and P. Verrocchio, Phys. Rev. Lett. **98**, 187801 (2007).

[10] G. Biroli, J.-P. Bouchaud, A. Cavagna, T. S. Grigera, and P. Verrocchio, Nat. Phys. **4**, 771 (2008).

[11] P. Scheidler, W. Kob, and K. Binder, Eur. Phys. J. E **12**, 5 (2003).

[12] S. Franz and A. Montanari, J. Phys. A: Math. Theor. **40**, F251 (2007).

[13] B. Zhang and X. Cheng, Phys. Rev. Lett. **116**, 098302 (2016).

[14] C. Balbuena, M. M. Gianetti, and E. R. Soulé, J. Chem. Phys. **150**, 234508 (2019).

[15] J. Baschnagel and F. Varnik, J. Phys.: Condens. Matter **17**, R851 (2005).

[16] E. Flenner and G. Szamel, Nat. Phys. **8**, 696 (2012).

[17] V. Krakoviack, Phys. Rev. E **75**, 031503 (2007).

[18] V. Vaibhav, J. Horbach, and P. Chaudhuri, Phys. Rev. E **101**, 022605 (2020).

[19] C. Lozano, J. R. Gomez-Solano, and C. Bechinger, Nat. Mater. **18**, 1118 (2019).

[20] B. Li, K. Lou, W. Kob, and S. Granick, Nature (London) **587**, 225 (2020).

[21] S. F. Swallen, K. L. Kearns, M. K. Mapes, Y. S. Kim, R. J. McMahon, M. D. Ediger, T. Wu, L. Yu, and S. Satija, Science **315**, 353 (2007).

[22] H.-B. Yu, Y. Luo, and K. Samwer, Adv. Mater. **25**, 5904 (2013).

[23] P. Luo, C. R. Cao, F. Zhu, Y. M. Lv, Y. H. Liu, P. Wen, H. Y. Bai, G. Vaughan, M. di Michiel, B. Ruta, and W. H. Wang, Nat. Commun. **9**, 1389 (2018).

[24] W. Kob and H. C. Andersen, Phys. Rev. E **51**, 4626 (1995).

[25] M. I. Mendelev, M. J. Kramer, R. T. Ott, D. J. Sordelet, D. Yagodin, and P. Popel, Phil. Mag. **89**, 967 (2009).

[26] S. Plimpton, J. Comp. Phys. **117**, 1 (1995).

[27] Supplemental Material.

[28] O. G. Shpyrko, A. Y. Grigoriev, C. Steimer, P. S. Pershan, B. Lin, M. Meron, T. Graber, J. Gerbhardt, B. Ocko, and M. Deutsch, Phys. Rev. B **70**, 224206 (2004).

[29] H. Mo, G. Evmenenko, S. Kewalramani, K. Kim, S. N. Ehrlich, and P. Dutta, Phys. Rev. Lett. **96**, 096107 (2006).

[30] J. Haddad, D. Pontoni, B. M. Murphy, S. Festersen, B. Runge, O. M. Magnussen, H.-G. Steinrueck, H. Reicher, B. M. Ocko, and M. Deutsch, Proc. Natl. Acad. Sci USA **115**, E1100 (2018).

[31] J. Gao, W. D. Luedtke, and U. Landman, Phys. Rev. Lett. **79**, 705 (1997).

[32] E. Chacón, M. Reinaldo-Falagán, E. Velasco, and P. Tarazona, Phys. Rev. Lett. **87**, 166101 (2001).

[33] K. S. Schweizer and D. S. Simmons, J. Chem. Phys. **151**, 240901 (2019).

[34] A. D. Phan and K. S. Schweizer, Macromolecules **52**, 5192 (2019).

[35] D. Diaz-Vela, J.-H. Hung, and D. S. Simmons, ACS Macro Lett. **7**, 1295 (2018).

[36] L. Berthier, G. Biroli, D. Coslovich, W. Kob, and C. Toninelli, Phys. Rev. E **86**, 031502 (2012).

[37] H. L. Peng and Th. Voigtmann, Phys. Rev. E **94**, 042612 (2016).

[38] S. Karmakar, C. Dasgupta, and S. Sastry, Phys. Rev. Lett. **105**, 019801 (2010).

[39] J. D. Stevenson, J. Schmalian, and P. G. Wolynes, Nat. Phys. **2**, 268 (2006).

[40] Y. Gebremichael, M. Vogel, and S. C. Glotzer, J. Chem. Phys. **120**, 4415 (2004).

[41] F. W. Starr, J. F. Douglas, and S. Sastry, J. Chem. Phys. **138**, 12A541 (2013).

[42] T. Nakayama and K. Yakubo, *Fractal Concepts in Condensed Matter Physics* (Springer, 2003).

[43] Y. Gebremichael, T. B. Schrøder, F. W. Starr, and S. C. Glotzer, Phys. Rev. E **64**, 051503 (2001).

[44] C. Donati, J. F. Douglas, W. Kob, S. J. Plimpton, P. H. Poole, and S. C. Glotzer, Phys. Rev. Lett. **80**, 2338 (1998).

[45] B. A. P. Betancourt, J. F. Douglas, and F. W. Starr, J. Chem. Phys. **140**, 204509 (2014).

[46] S. Sengupta, S. Karmakar, C. Dasgupta, and S. Sastry, J. Chem. Phys. **138**, 12A548 (2013).

[47] T. Kawasaki and A. Onuki, Phys. Rev. E **87**, 012312 (2013).

[48] S. C. Glotzer, V. N. Novikov, and T. B. Schroder, J. Chem. Phys. **112**, 509 (2000).

[49] S. Sengupta, S. Karmakar, C. Dasgupta, and S. Sastry, J. Chem. Phys. **140**, 224505 (2014).

[50] H. R. Schober and H. L. Peng, Phys. Rev. E **93**, 052607 (2016).

[51] T. Rizzo, Phys. Rev. E **87**, 022135 (2013).

[52] T. Rizzo, EPL **106**, 56003 (2014).

[53] T. Rizzo, Phys. Rev. B **94**, 014202 (2016).

[54] T. Rizzo and T. Voigtmann, EPL **111**, 56008 (2015).